Development of the Poplar-Laccaria bicolor Ectomycorrhiza Modifies Root Auxin Metabolism, Signaling, and Response

Alice Vayssieres, Ales Pěnčík, Judith Felten, Annegret Kohler, Karin Ljung, Francis Martin, Valerie Legue

Development of the Poplar-*Laccaria bicolor* Ectomycorrhiza Modifies Root Auxin Metabolism, Signaling, and Response[1]

Alice Vayssières, Ales Pěnčík, Judith Felten, Annegret Kohler, Karin Ljung, Francis Martin, and Valérie Legué[2]*

Institut National de la Recherche Agronomique and Université de Lorraine, Unité Mixte de Recherche Interactions Arbres/Microorganismes 1136, Institut National de la Recherche Agronomique-Nancy, F–54280 Champenoux, France (A.V., J.F., A.K., F.M., V.L.); and Umeå Plant Science Centre, Department of Forest Genetics and Plant Physiology, Swedish University of Agricultural Sciences, 901 83 Umea, Sweden (A.P., K.L.)

ORCID IDs: 0000-0002-0444-822X (J.F.); 0000-0003-2901-189X (K.L.); 0000-0002-4737-3715 (F.M.).

Root systems of host trees are known to establish ectomycorrhizae (ECM) interactions with rhizospheric fungi. This mutualistic association leads to dramatic developmental modifications in root architecture, with the formation of numerous short and swollen lateral roots ensheathed by a fungal mantle. Knowing that auxin plays a crucial role in root development, we investigated how auxin metabolism, signaling, and response are affected in poplar (*Populus* spp.)-*Laccaria bicolor* ECM roots. The plant-fungus interaction leads to the arrest of lateral root growth with simultaneous attenuation of the synthetic auxin response element *DR5*. Measurement of auxin-related metabolites in the free-living partners revealed that the mycelium of *L. bicolor* produces high concentrations of the auxin indole-3-acetic acid (IAA). Metabolic profiling showed an accumulation of IAA and changes in the indol-3-pyruvic acid-dependent IAA biosynthesis and IAA conjugation and degradation pathways during ECM formation. The global analysis of auxin response gene expression and the regulation of *AUXIN SIGNALING F-BOX PROTEIN5*, *AUXIN/IAA*, and *AUXIN RESPONSE FACTOR* expression in ECM roots suggested that symbiosis-dependent auxin signaling is activated during the colonization by *L. bicolor*. Taking all this evidence into account, we propose a model in which auxin signaling plays a crucial role in the modification of root growth during ECM formation.

Root systems of most plants display symbiosis with mutualistic fungi, which are essential for nutrient acquisition and plant development. In boreal and temperate forests, the most common rhizospheric symbioses are ectomycorrhizae (ECM), a dynamic relationship between roots of host trees and hyphae of certain Basidiomycota or Ascomycota species (Smith and Read, 2008). The fungal hyphae colonize lateral root (LR) tips of host trees and form an ECM root, a new composite organ that becomes the site of mutualistic interactions between the two symbionts (Martin and Nehls, 2009). Some ECM root tips have a recognizable phenotype made of (1) an extensive extramatrical hyphae network prospecting the soil, (2) a mantle of aggregated hyphae that form a sheath-like storage compartment around rootlets, and (3) the Hartig net, a network of hyphae growing intercellularly between epidermal and cortical cells, where nutrients and carbohydrates are exchanged (Massicotte et al., 1987). The formation of ECM roots involves a chain of complex and overlapping developmental processes in the plant host, including the formation of new LRs (Burgess et al., 1996; Tranvan et al., 2000; Niemi et al., 2002; Rincón et al., 2003; Felten et al., 2009; Splivallo et al., 2009), radial expansion of epidermal cells in angiosperm hosts, root hair decay (Horan et al., 1988; Ditengou et al., 2000), and a reduction in the size of the root cap (Massicotte et al., 1987). Together, these morphological changes lead to the characteristic short-root phenotype of ECM roots. This is only a broad definition of the ECM phenotype, as the precise changes in morphology vary according to the host plant. For example, *Tuber* spp. were found to inhibit *Cistus incanus* root growth (Splivallo et al., 2009), whereas primary root growth increased as a response to *Laccaria bicolor* in *Picea abies* and to *Hebeloma cylindrosporum* in *Pinus pinaster* (Karabaghli et al., 1998; Tranvan et al., 2000). In *Pinus densiflora*, the ECM fungal species, *Pisolithus* sp. and *Cenoccum geophilum*, differ in their induction of root growth (Rathnayake et al., 2008).

It is well established that root development is regulated by cross-talk between plant hormones, with auxin being a master regulator (Parizot and Beeckman, 2013). Local auxin accumulation at the root apex is central to its action in root growth (Tanaka et al., 2006). Auxin levels are maintained in response to environmental and developmental conditions by complex and robust networks that positively and/or negatively regulate indole-3-acetic acid (IAA) metabolism, auxin transport, and auxin signaling (Rosquete et al., 2012). Trp-dependent pathways are the principal routes of IAA biosynthesis (Ljung, 2013). There is genetic and biochemical evidence that IAA biosynthesis can occur

with the amino acid Trp as precursor through four pathways, the indole-3-pyruvic acid (IPyA), indole-3-acetamide (IAM), tryptamine (TRA), and indole-3-acetaldoxime (IAOx) pathways (Ljung, 2013). IAA is also metabolized through conjugation, mainly to amino acids and sugars (Ludwig-Müller, 2011), and degradation (Peer et al., 2013; Pencík et al., 2013).

Auxin is perceived by a coreceptor module consisting of an F-box protein from the TRANSPORT INHIBITOR RESPONSE1/AUXIN SIGNALING F-BOX PROTEIN (TIR1/AFB) family and a member of the AUXIN/INDOLE ACETIC ACID (Aux/IAA) family of transcriptional regulators (Dharmasiri et al., 2005; Kepinski and Leyser, 2005). Aux/IAA proteins can dimerize with one another or with AUXIN RESPONSE FACTORS (ARFs; Fukaki et al., 2005; Dreher et al., 2006). When auxin levels are low, Aux/IAA proteins bind to ARFs and repress their transcriptional activity. On the other hand, the presence of auxin promotes interaction between the two components TIR1/AFB and Aux/IAA, leading to the ubiquitination and 26S proteasome-mediated degradation of the latter, thus activating the transcriptional response (Dharmasiri et al., 2005; Kepinski and Leyser, 2005). In Arabidopsis (*Arabidopsis thaliana*), the combinatorial interactions between six TIR1/AFBs, 29 Aux/IAAs, and 23 ARFs result in a large diversity of coreceptors, contributing to the complexity of auxin responses throughout plant growth and development and determining dynamic auxin-sensing properties (Vernoux et al., 2011; Calderón-Villalobos et al., 2012).

Microorganisms interacting with plants often manipulate the hormonal homeostasis of the host to facilitate their colonization (Sukumar et al., 2013). Auxin is thought to play a central role in mycorrhizal developmental pathways, as significant changes in auxin signaling and the expression of auxin-responsive genes have been detected at different stages of ECM root differentiation (Charvet-Candela et al., 2002; Reddy et al., 2006; Felten et al., 2009; Heller et al., 2012; Flores-Monterroso et al., 2013; Tarkka et al., 2013). The interaction between an IAA-overproducing mutant of the ECM fungus *H. cylindrosporum* with *Pinus pinaster* root tissues led to an increase in fungal colonization compared with the fungal wild type. The presence of 2,3,5-triiodobenzoic acid, an inhibitor of polar auxin transport, completely prevented root colonization. These studies led to the hypothesis that auxin is a key regulator during formation of the Hartig net (Gay et al., 1994; Tranvan et al., 2000). Conversely, other studies have demonstrated lower IAA levels in ECM roots than in noncolonized roots of poplar (*Populus* spp.) and spruce (*Picea* spp.; Wallander et al., 1992; Luo et al., 2009). There is a decrease in expression of the auxin-induced soybean (*Glycine max*) *GH3* genes, which code for orthologs of putative IAA-conjugating enzymes, in *Pinus* spp. ECM roots (Reddy et al., 2006; Heller et al., 2012). In transgenic *GH3*::*GUS Populus* spp. lines, reporter gene expression was absent in the roots of *Populus* × *canescens-Paxillus involutus* ECM (Luo et al., 2009). These results suggest that auxin is involved in symbiotic organ formation and that ECM roots have low auxin levels. However, the multiple roles of auxin during ECM development are not yet fully understood.

In this study, we assessed auxin metabolism, signaling, and molecular responses during the development of ECM roots of *Populus tremula* × *Populus alba* interacting with the symbiotic basidiomycete *L. bicolor* (Martin et al., 2008). Our results show that *Populus* spp. root growth was arrested during colonization by *L. bicolor*. *DR5*::*GUS* expression in these roots outlined an impaired auxin response in plant tissues during the establishment of the mycorrhizal symbiosis. The auxin-related metabolite profiling revealed an accumulation of IAA and changes in IPyA-dependent IAA biosynthesis as well as increases of IAA conjugation and degradation pathways during ECM formation. Finally, our transcriptome study of mature ECM provided evidence for symbiosis-dependent auxin signaling.

RESULTS

Development of *Populus* spp.-*L. bicolor* ECM Leads to Root Growth Arrest

Colonization of *P. tremula* × *P. alba* roots by *L. bicolor* mycelium leads to profound changes in root architecture (Fig. 1, A and B). In this study, we quantified the effect of colonization of LRs and ARs by *L. bicolor* on

[1] This work was supported by the French National Research Agency through the Laboratory of Excellence ARBRE (grant no. ANR–11–LBX–002–01), the European Commission Project EnergyPoplar (grant no. FP7–211917), the Plant-Microbe Interactions Project, Genomic Science Program, of the U.S. Department of Energy, Office of Science, Biological, and Environmental Research (grant no. DE–AC05–00OR22725), the Centre National d'Etudes Spatiales, the Institut National de la Recherche Agronomique, the Région de Lorraine, and the European Fund for Regional Development (funding for the Functional Genomics Facilities at Institut National de la Recherche Agronomique-Nancy), the Université de Lorraine (fellowship to A.V.), and the Swedish Governmental Agency for Innovation Systems, the Swedish Research Council, and the Kempe Foundation (to K.L. and A.P.).

[2] Present address: Université Blaise Pascal and Institut National de la Recherche Agronomique, Unité Mixte de Recherche 547, Physique et Physiologie intégratives de l'Arbre Fruitier et Forestier, Campus Universitaire des Cézeaux, 8 Avenue Blaise Pascal, 63178 Aubiere cedex, France.

* Address correspondence to valerie.legue@univ-bpclermont.fr.

The author responsible for distribution of materials integral to the findings presented in this article in accordance with the policy described in the Instructions for Authors (www.plantphysiol.org) is: Valérie Legué (valerie.legue@univ-bpclermont.fr).

A.V. designed the study, performed the experiments, analyzed all the data, and wrote the article with contributions of all the authors; A.P. performed the quantification of IAA-related compounds; J.F. provided advice to A.V. and performed specific experiments; A.K. supervised and contributed the analysis of whole-genome expression oligoarray; K.L. supervised the quantification of IAA-related compounds; F.M. designed the study, supervised the experiments, and edited the article; V.L. designed the study, supervised the experiments, analyzed the data, and contributed to the writing and editing of the article with contributions of all the authors.

www.plantphysiol.org/cgi/doi/10.1104/pp.114.255620

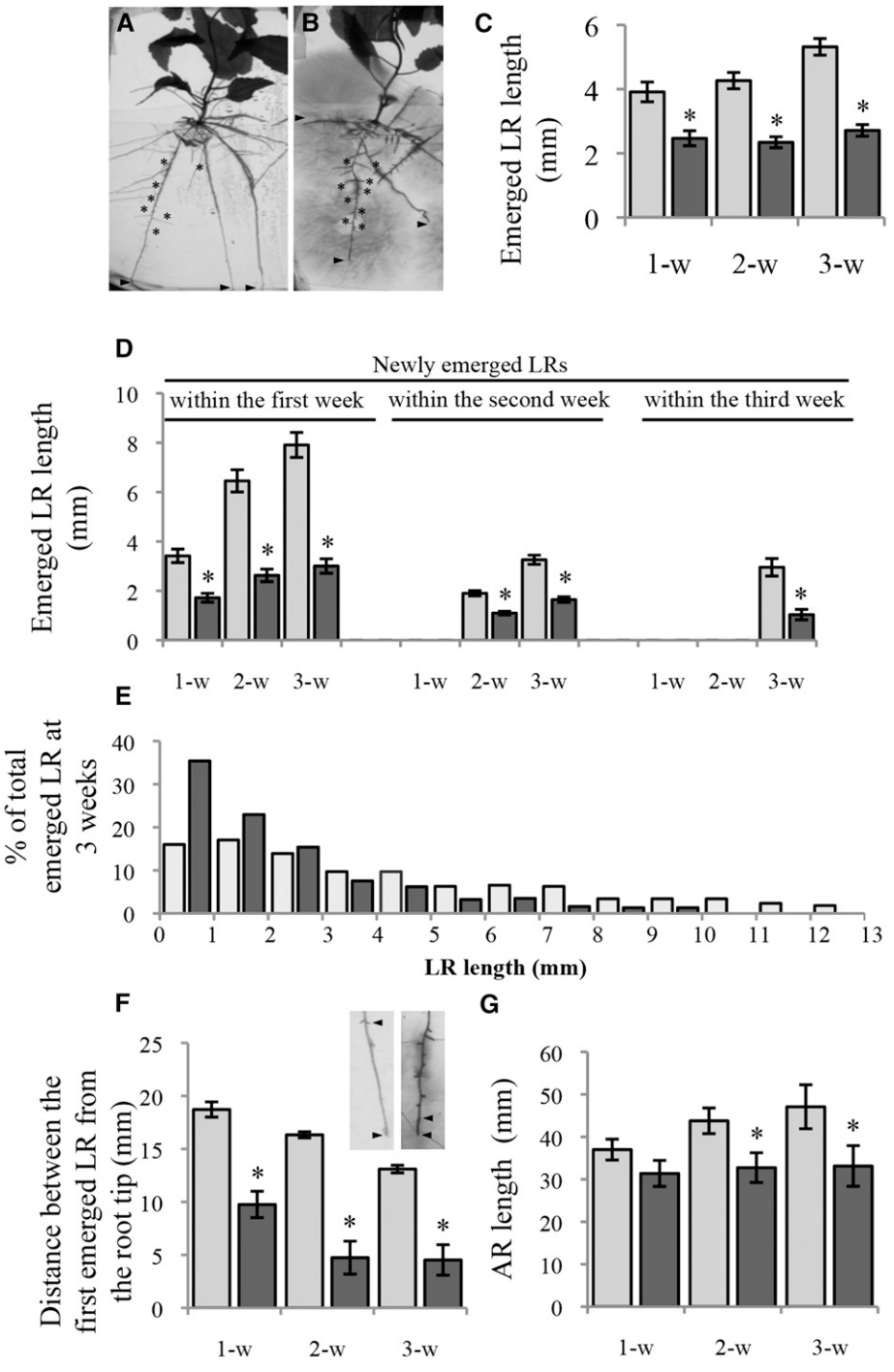

Figure 1. *L. bicolor* colonization induced root growth arrest of the *P. tremula* × *P. alba* host. A and B, Root system architecture of *P. tremula* × *P. alba* grown in the absence of *L. bicolor* (A) and after 3 weeks of *L. bicolor* coculture (B). Asterisks indicate typical LRs or ECM roots in A and B, respectively, and arrowheads indicate adventitious roots (ARs). C, Mean LR length after 1, 2, and 3 weeks (-w) of culture in the absence (gray bars) or in the presence of *L. bicolor* (black bars). D, Mean lengths of newly emerged LRs after 1 week (n = 136–160), 2 weeks (n = 168–198), and 3 weeks (n = 22–55) of culture in the absence (gray bars) or in the presence of *L. bicolor* (black bars). E, Distribution of LR root length as a proportion of the total number of LRs after 3 weeks of culture in the absence (gray bars; n = 370) or in the presence of *L. bicolor* (black bars; n = 380). LR length classes that made up less than 1% of the total LRs are not indicated. F, Mean distance between the first visible emerging LRs from the apex of the parental root (n = 8 plants). Insets show photographs of representative phenotypes after 3 weeks in the absence (left) or in the presence of *L. bicolor* (right). G, Mean AR length (n = 8 plants) of *Populus* spp. grown in the absence (gray bars) or in the presence of *L. bicolor* (black bars) after 1, 2, and 3 weeks. Asterisks indicate significant differences between control and cocultured roots (Student's t test according to F test, $P < 0.05$).

root growth. After 1 week of fungus-plant coculture, the mean LR length was significantly reduced as compared with control roots grown without *L. bicolor* (Fig. 1C). We analyzed the growth of LRs that had newly emerged during the time course of fungal colonization (Fig. 1D). LRs that emerged in the presence of *L. bicolor* within the first week of coculture showed greater than 50% reduction in length when compared with LRs that emerged in the absence of the fungus during the same period. *L. bicolor* also inhibited the growth of LRs that emerged during the second and third weeks of coculture. Interestingly, the mean length of newly emerged LRs within the first week remained constant within the second and third weeks of fungus-plant coculture, whereas control LR length increased (Fig. 1D). These results emphasize that ECM development leads to the arrest of LR growth in *P. tremula* × *P. alba* -*L. bicolor* ECM. After 3 weeks of coculture, around

60% of ECM LRs were short (less than 2 mm) compared with 33% of control roots (Fig. 1E). Therefore, the arrest of LR root growth led to the typical short-root phenotype after 3 weeks of coculture, a time point that corresponds to the mature ECM stage in most roots (Felten et al., 2009).

We also investigated whether *L. bicolor* colonization induced a change in AR growth. After 3 weeks of culture, the first visible emerged LR from the root tip was observed 13 mm from the apex of the AR in the control root systems, whereas the first visible emerged LR in the root systems colonized by *L. bicolor* was 4 mm from the AR apex (Fig. 1F). The mean length of ARs after 3 weeks of coculture was 30% shorter than that of control ARs (Fig. 1G), suggesting that the interaction with *L. bicolor* induced a subsequent arrest of AR growth. These results are clear evidence that mechanisms regulating LR growth and AR growth are modified during ECM root formation in the in vitro *P. tremula* × *P. alba*-*L. bicolor* system.

The DR5-Related Auxin Response Is Altered during ECM Root Growth Arrest

We investigated the DR5-related auxin response in root apices of transgenic *P. tremula* × *P. alba* transformed with the auxin-inducible promoter-reporter construct *DR5*::*GUS* (Sabatini et al., 1999; Ulmasov et al., 1999) during colonization by *L. bicolor*. *DR5*-directed *GUS* expression in *P. tremula* × *Populus tremuloides* control roots was restricted to the root apex, including root cap cells and the quiescent center (Fig. 2A). Two stages of colonization were observed after 2 weeks of coculture with *L. bicolor*. (1) The presence of a dense fungal mycelium sheath surrounding the flanks of the root before the Hartig net is established is referred to as the colonized root stage (Fig. 2B). At this stage, the area of GUS expression was significantly smaller than in the control (Fig. 2, B and E). (2) The second stage was characterized by a well-developed fungal sheath around the entire root with a visible Hartig net, here referred to as mature ECM (Fig. 2C). The *Populus* spp. ECM showed the distinctly swollen appearance typical for ECM roots (Massicotte et al., 1987; Horan et al., 1988). The *GUS* expression pattern at this stage was only visible in a few cells around the quiescent center (Fig. 2, C and E). No GUS expression was observed in the epidermal cells at the interface of the root with *L. bicolor* hyphae (Fig. 2D). Auxin was applied to *DR5*::*GUS* roots. As expected, application of auxin (10 μM IAA or 10 μM α-naphthalene acetic acid [NAA] for 16 h) to control roots increased the ectopic expression of *DR5*::*GUS* in the entire LR, including the root meristem and elongation zone (Fig. 2, G and H). In contrast, auxin application to mature ECM root tips did

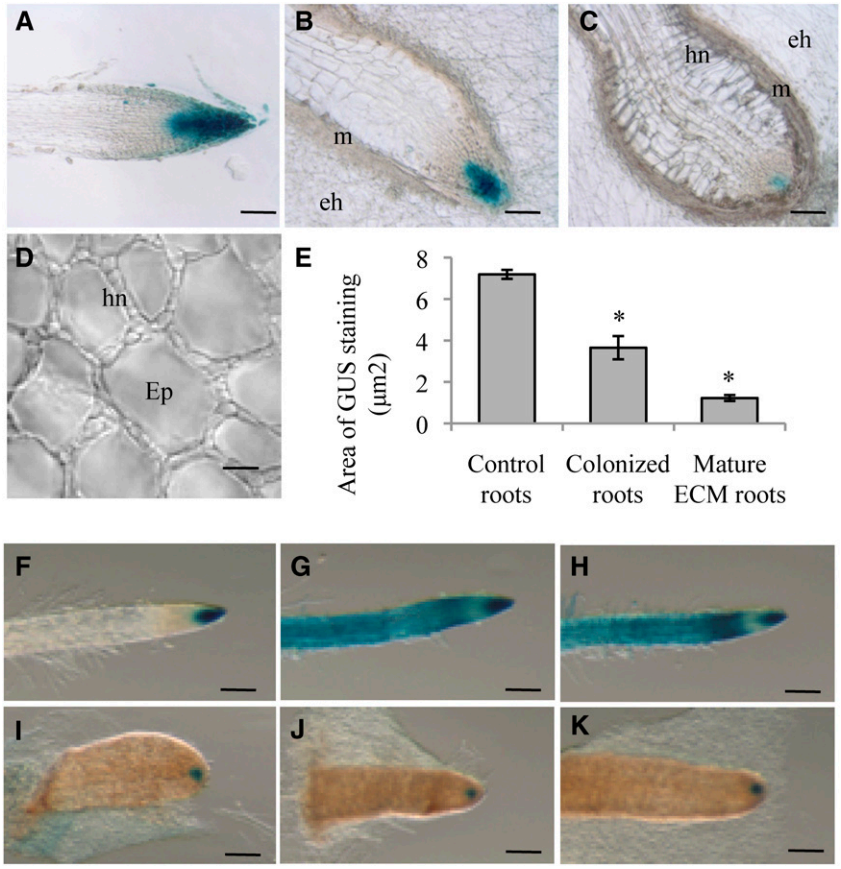

Figure 2. The DR5 auxin response is attenuated in mature ECM. A to C, Spatial expression patterns of GUS activity in longitudinal root sections of *P. tremula* × *P. tremuloides DR5*::*GUS* plant roots grown for 2 weeks in the absence (A) or presence (B and C) of *L. bicolor*. D, Apical root sections of a colonized root (B) and a mature ECM root (C) show visible Hartig net (hn) between epidermal cells. E, Mean areas of GUS staining in control roots (n = 3), colonized roots (n = 10), and mature ECM roots (n = 10). Asterisks indicate significant differences between control and cocultured roots (Student's t test according to F test, $P < 0.05$). F to K, Spatial expression patterns of GUS activity in *P. tremula* × *P. tremuloides DR5*::*GUS* roots grown for 2 weeks in the absence (F–H) or in the presence (I–K) of *L. bicolor*. Roots were then incubated for 16 h in growth medium without auxin (F and I) or in growth medium containing 10 μM IAA (G and J) or 10 μM NAA (H and K). Images show typical roots among 20 replicates for each condition. eh, Extramatrical hyphae; Ep, epidermal cell; m, fungal mantle. Bars = 50 μm (A–C), 150 μm (D), and 0.1 mm (F–K).

not change the *GUS* expression pattern (Fig. 2, J and K); GUS staining remained localized to the same restricted zone.

Thus, a significant decrease in GUS expression in both colonized and mature ECM root tips (Fig. 2E) and the absence of auxin induction of GUS expression show that the DR5-related auxin response is impaired in roots by ECM formation.

ECM Partners Have Distinct IAA Metabolite Profiles

IAA and 11 IAA metabolites (precursors, catabolites, and conjugates) from free-living mycelium of *L. bicolor* and *P. tremula* × *P. alba* root apices were quantified by liquid chromatography/multiple reaction monitoring/mass spectrometry (Fig. 3). The average concentration of free IAA was 49 pg mg^{-1} fresh weight in free-living *L. bicolor*. The IAA precursors anthranilate (ANT) and Trp were detected. Among metabolites related to the Trp-dependent biosynthesis pathway, IPyA concentrations were higher than TRA concentrations, and the level of IAOx, IAM, and indole-3-acetonitrile were below the detection limit. IAA conjugates, such as IAA-Asp (IAAsp) and IAA-Glu (IAGlu), were not detected in *L. bicolor* mycelium. Instead, the IAA catabolite 2-oxoindole-3-acetic acid (oxIAA) was detected in *L. bicolor* mycelium at 0.4 pg mg^{-1} fresh weight. Addition of 10 μM IAA to *L. bicolor* growth medium induced an 8-fold increase in the IAA concentration and a 4-fold increase in the oxIAA concentration compared with control mycelium (Supplemental Fig. S1), while the IAA conjugates were still below the detection limit. Exogenous IAA treatment also caused a decrease in the levels of the IAA precursors ANT, Trp, and IPyA, possibly due to feedback inhibition of specific IAA biosynthesis pathways (Supplemental Fig. S1). These IAA metabolite profiles showed that *L. bicolor* mycelium was characterized by an elevated content of free IAA. The abundance of the IAA precursors ANT and IPyA is an indicator for a high rate of IAA biosynthesis in the mycelium.

The IAA biosynthesis pathways in *Populus* spp. have so far not been elucidated; therefore, we decided to quantify in control root apices of *P. tremula* × *P. alba* all the major known IAA metabolites that have been identified in Arabidopsis and other plant species (Novák et al., 2012; Ljung, 2013). The free IAA level

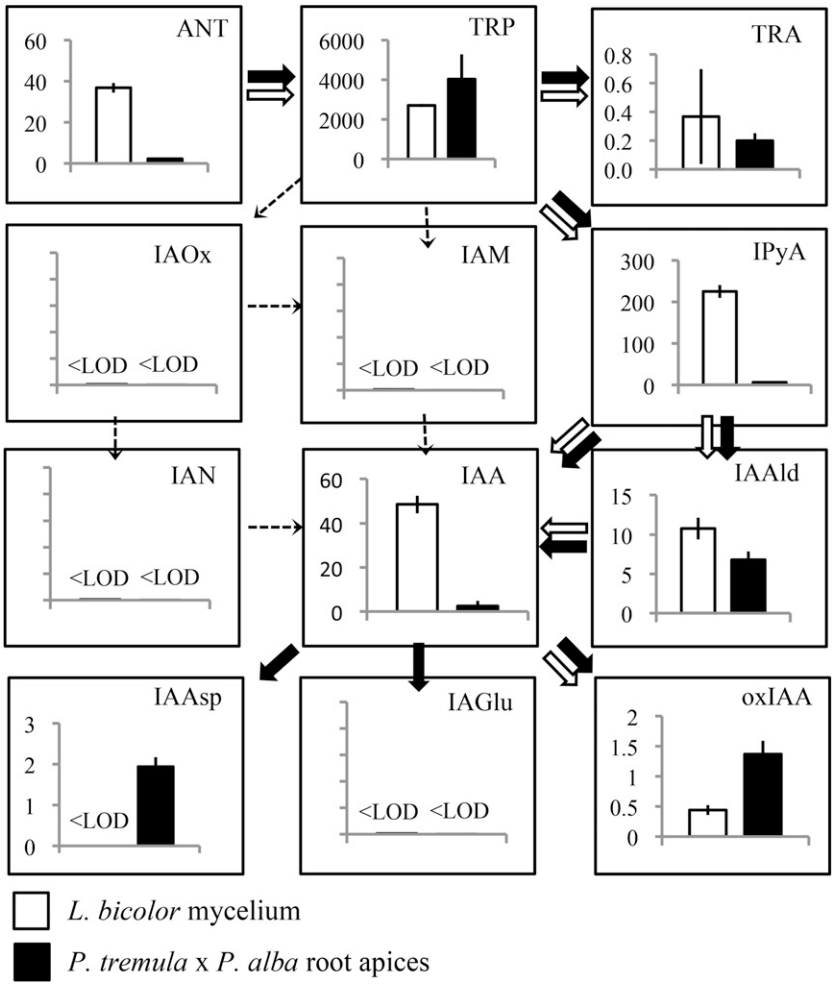

Figure 3. Auxin-related metabolites in free-living *L. bicolor* mycelium and in *P. tremula* × *P. alba* root apices. The concentrations (pg mg^{-1} fresh weight) of auxin-related metabolites in free-living *L. bicolor* mycelium (white bars) and in *P. tremula* × *P. alba* root apices (black bars), grown separately for 10 d or 3 weeks, respectively, are shown. White and black arrows indicate the deduced IAA metabolism pathways in *L. bicolor* hyphae and *Populus* spp. root tips, respectively (according to Ljung, 2013). Dashed arrows indicate metabolic pathways for which metabolites were under the limit of detection (<LOD) in the samples analyzed. IAN, Indole-3-acetonitrile.

was 2.5 pg mg^{-1} fresh weight (Fig. 3). Precursors of IAA biosynthesis including ANT and Trp were detected. TRA and IPyA, intermediates of Trp-dependent pathways, were found, but IAOx, IAM, and indole-3-acetonitrile were not detected in root apices (Fig. 3; Supplemental Table S1) or in *Populus* spp. leaves (Supplemental Table S1). Only metabolites of TRA- and IPyA-dependent biosynthesis pathways were detected in *Populus* spp. root tips. The major degradation product of IAA in Arabidopsis is oxIAA (Novák et al., 2012), and this molecule was found in *Populus* spp. roots as well as the conjugated product IAAsp. IAGlu was undetectable in control root apices of *Populus* spp. but was detected in the tips of younger roots (Supplemental Table S1).

Auxin-Related Metabolite Changes in Both Partners during ECM Interaction

We profiled IAA and its related metabolites in *Populus* spp.-*L. bicolor* composite organs at 1 and 3 weeks of coculture, as these time points are considered to capture the two important steps of the ECM-dependent root growth modulation (Figs. 1 and 2). We furthermore analyzed auxin metabolites in the extramatrical *L. bicolor* mycelium expanding from ECM roots (after 1 and 3 weeks of coculture) as well as in free-living mycelium (grown independently of the plant partner) and in roots cocultured with *L. bicolor* but without direct physical contact (1 week with a cellophane membrane separating the two partners).

To better pinpoint the major differences in IAA metabolite profiles from the different organisms, compartments, and colonization stages, a principal component analysis was used to evaluate all the data generated (Fig. 4, A and B). The first two components of the model explained 60% of the total variance. A component scores plot for principal components PC1 and PC2 strongly differentiated auxin-associated metabolite changes during the formation of mature ECM (Fig. 4A). The first component (PC1) of the model explained 33% of the variance and discriminates

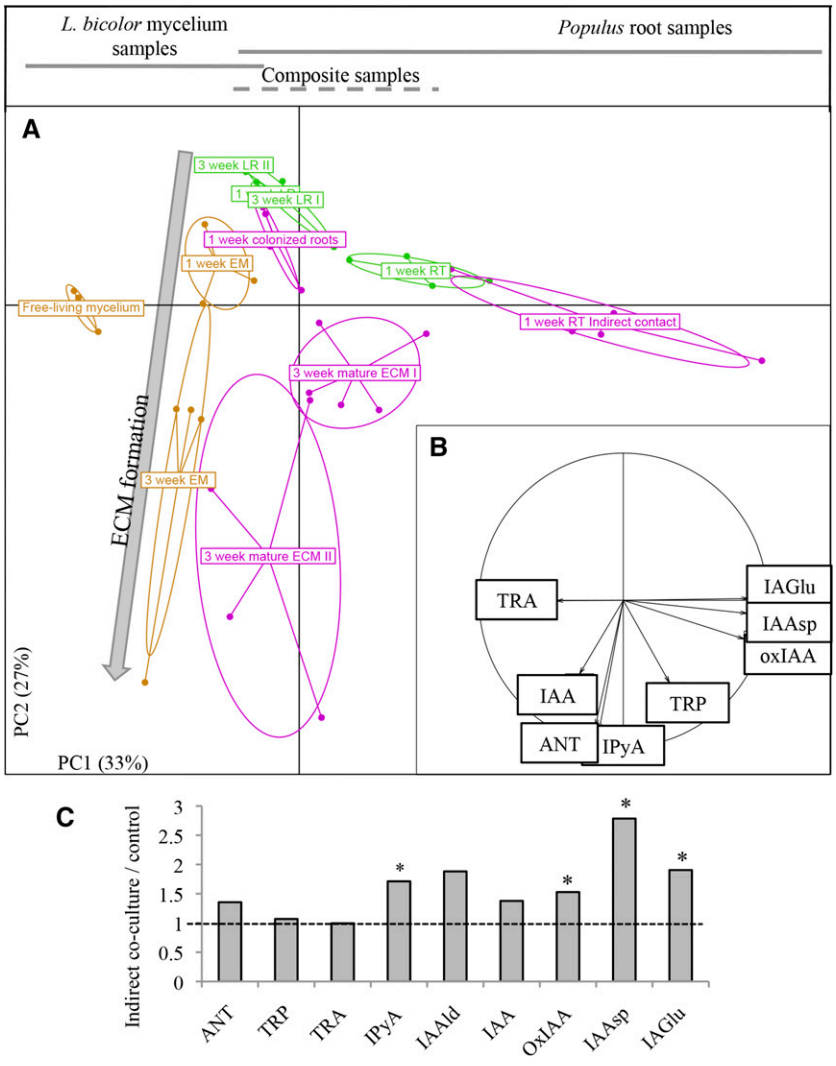

Figure 4. Multivariate analysis reveals the changes of auxin-related metabolite levels during ECM development. A, Principal component analysis plot showing the positions of samples in the plane delineated by PC1 and PC2 accounting for 60% of the total variance between auxin metabolite concentrations. The indole-3-acetaldehyde (IAAld) concentration was not included in the analysis, as it was under the limit of detection in the majority of samples. Different colors illustrate the different conditions studied as follows: magenta, samples from *Populus* spp. roots at the colonized stage (after 1 week of coculture with *L. bicolor*), at the mature ECM stage (after 3 weeks of coculture) from two independent biological experiments I and II, and controls after 1 week of coculture without physical contact with *L. bicolor*; green, control LR samples and control root tip (RT) samples; and brown, samples from extramatrical mycelium (EM) grown for 1 or 2 weeks or from free-living mycelium. The image at top shows hypothetical sample segregation in PC1. The large gray arrow shows a hypothetical shift in the composition of auxin-related metabolites during ECM formation in PC2. B, Correlation circle displays auxin-related metabolites showing discrimination between samples in the component plot (A). C, Concentration ratios between auxin-related metabolites in root apices after 1 week of indirect coculture (through a cellophane membrane) compared with those in control conditions. Asterisks indicate significant differences between control and coculture roots with Student's *t* test according to *F* test, $P < 0.05$ ($n = 5$).

L. bicolor samples from *Populus* spp. roots without *L. bicolor* samples (Fig. 4A, top square), due to the high TRA concentration in free-living mycelium and the presence of IAGlu, IAAsp, and oxIAA in *Populus* spp. root tips (Fig. 4B). This confirms our previous statement (Fig. 3) that each partner has a distinct metabolite profile. The second component (PC2) accounted for 27% of the variance between samples clearly and gradually discriminates nonmycorrhizal LRs from colonized roots of mature ECM (independent experiments I and II; Fig. 4A), due to gradually increasing IAA, ANT, IPyA, and Trp concentrations during ECM formation (Fig. 4B). Interestingly, the principal component analysis revealed that the metabolite profile of extramatrical mycelium is more similar to the metabolite profile of colonized roots or mature ECM than to free-living mycelium (Fig. 4A). This indicates that IAA metabolites are affected when the mycelium interacts with *Populus* spp. roots. In addition to this multivariate analysis, the ratio of concentrations for each metabolite from *Populus* spp. roots grown without physical contact with *L. bicolor* versus control LRs (Fig. 4C) was calculated. No significant change in IAA concentrations was observed, but higher concentrations of IPyA, oxIAA, IAAsp, and IAGlu were detected when roots were exposed to *L. bicolor* mycelium through a membrane.

In conclusion, these results highlight a change in the IAA concentration during ECM formation and distinct modifications in IAA metabolites in *L. bicolor* hyphae and in *Populus* spp. roots.

ECM Arrest of Root Growth Is Associated with Changes in Auxin-Related Gene Expression

To determine possible molecular mechanisms such as changes in auxin biosynthesis, signaling, and responses that could cause the morphological and metabolic changes observed, an array-based transcript profiling was performed comparing 3-week-old ECM with control LRs. A total of 7,091 *Populus* spp. transcripts, corresponding to 16% of the predicted gene models in the *Populus trichocarpa* V2 gene repertoire (43,929 genes), were differentially expressed (greater than 2-fold change, with Benjamini and Hochberg-corrected ANOVA $P < 0.05$) in ECM compared with control LRs (Supplemental Table S2). Among these transcripts, 60% (4,256 genes) accumulated during ECM formation. From the 2,835 repressed transcripts, 38% (1,072 genes) were expressed in control LRs but were not detected in ECM roots. This indicates a profound reorganization of gene expression in mature ECM roots. The study revealed among ECM-regulated genes several with homology to genes that, in Arabidopsis, are associated with the development of the root meristem and whose proteins regulate the biosynthesis, degradation, and signaling of auxin, cytokinin, GA, or brassinosteroids (Table I; Supplemental Table S3; Depuydt and Hardtke, 2011).

We also studied whether ECM-regulated genes overlapped significantly with IAA-regulated genes identified in published studies. Randomization tests (see "Materials and Methods") were used to compare the ECM-regulated gene set with an Arabidopsis IAA-regulated gene set (I; Nemhauser et al., 2006) and an IAA-induced gene set from auxin-responsive genes in *Populus* spp. woody stem tissues (II; Nilsson et al., 2008). Sets I and II were compared with each other ($P = 0$) and with the set of differentially expressed genes of ECM roots (Fig. 5A). There was a significant overlap of ECM-regulated genes with auxin-response genes from both sets I and II ($P \leq 0.001$; Fig. 5A). We confirmed the auxin responsiveness of a few selected ECM-regulated targets by quantitative real-time PCR and found that *PtaGH3-1*, *PtaIAA3.3*, and *PtaIAA20.2* responded with transcript accumulation to 2- and 6-h application of 10 μM IAA, while *PtaIAA28.1* levels decreased in these treatments (Supplemental Fig. S2). The nature of the transcript change (increase or decrease) during ECM formation or IAA treatment (set I) was compared. One hundred forty genes showed a change in their expression in the same direction (with transcripts being either increased or decreased by both IAA treatment and in ECM), and 183 genes showed an opposite response pattern (Fig. 5B; Supplemental Table S4). The dramatic alteration in the expression of auxin-response genes in mature ECM indicates that a specific auxin response is implemented during *L. bicolor* colonization.

Certain of the differentially expressed genes are implicated in the perception or transmission of the IAA signal (Table I). Two transcripts coding for *Populus* spp. proteins orthologous to AtAFB5, *Potri.005G159300.1* and *Potri.002G102700.1*, were increased in mature ECM roots compared with control LRs (Table I). In addition, seven members of the *PtaAux/IAA* family and two members of the *PtaARF* family (*PtaIAA3.3*, *PtaIAA3.4*, *PtaIAA12.1*, *PtaIAA15*, *PtaIAA20.2*, *PtaIAA28.1*, *PtaIAA28.2*, *PtaARF2.4*, and *PtaARF17.2*; Kalluri et al., 2007) were differentially expressed in ECM roots compared with LRs. These data suggest that the auxin-sensing pathway is modified in mature ECM. As expected from the auxin metabolite profile (Fig. 4), the abundance of transcripts coding for proteins involved in the IPyA-dependent IAA biosynthesis pathway (*PtaTAA1* and *PtaYUCCAs*) was modified in ECM as compared with control LRs. In addition, the expression level of *PtaGH3-1* and *PtaGH3-2*, which encode for acyl-amido synthases, was induced in ECM, while the *PtaGH3-7* expression level was repressed (Table I). The expression levels of *PtaPIN1c*, *PtaPIN3a*, *PtaPIN3b*, *PtaAUX2/LAX1*, and *PtaABCB19*, all coding for putative auxin transport carriers, were increased, whereas the expression levels of *PtaPIN2*, *PtaAUX8/LAX4*, *PtaAUX8/LAX8*, and *PtaABCB5* were decreased (Table I; Carraro et al., 2012; Liu et al., 2014). The differential expression of several of these genes (*PtaGH3-1*, *PtaIAA20.2*, *PtaIAA28.1*, *PtaIAA12.1*, and *PtaIAA3.4*) was confirmed by quantitative real-time

Table I. *Auxin-related genes regulated in mature ECM compared with control LRs*

nd, Under the average range of detection.

Gene Name[a]	Gene Identifier[b]	Arabidopsis Gene Identifier[c]	Arabidopsis Gene Name[c]	Fold Change Expression[d]	Expression in Control Roots[e]	Annotation[f]
Auxin signaling pathway						
	Potri.005G159300.1	*AT5G49980.1*	*AtAFB5*	3.37	906	IAA-signaling F box
	Potri.002G102700.1	*AT5G49980.1*	*AtAFB5*	2.33	791	IAA-signaling F box
PtaIAA3.4	*Potri.005G218200.1*	*AT5G43700.1*	*AtIAA4*	−5.62	1,593	IAA-signaling transcription regulator
PtaIAA3.3	*Potri.002G045000.1*	*AT5G43700.1*	*AtIAA4*	−12.71	701	IAA-signaling transcription regulator
PtaIAA28.2	*Potri.006G236200.1*	*AT3G16500.1*	*AtIAA26*	−3.21	3,808	IAA-signaling transcription regulator
PtaIAA28.1	*Potri.018G057000.1*	*AT3G16500.1*	*AtIAA26*	−4.40	3,299	IAA-signaling transcription regulator
PtaIAA20.2	*Potri.014G111700.1*	*AT3G62100.1*	*AtIAA30*	3.60	379	IAA-signaling transcription regulator
PtaIAA15	*Potri.001G177400.1*	*AT3G04730.1*	*AtIAA16*	4.43	1,651	IAA-signaling transcription regulator
PtaIAA12.1	*Potri.008G172400.1*	*AT2G33310.1*	*AtIAA13*	2.56	2,025	IAA-signaling transcription regulator
PtaARF2.4	*Potri.002G089900.1*	*AT1G77850.1*	*AtIAA17*	8.17	nd	IAA-signaling transcription factor
PtaARF17.2	*Potri.005G171300.1*	*AT1G77850.1*	*AtIAA17*	10.2	nd	IAA-signaling transcription factor
IAA biosynthesis/conjugation/degradation pathway						
PtaTAA1	*Potri.010G044500.1*	*AT1G70560.1*	*AtTAA1*	−6.28	1,281	Catalyzes conversion of Trp to IPyA
	Potri.006G248200.1	*AT5G11320.1*	*AtYUCCA4*	−2.63	331	Catalyzes conversion of IPyA to IAA
	Potri.006G243400.1	*AT5G25620.1*	*AtYUCCA6*	8.23	nd	Catalyzes conversion of IPyA to IAA
PtaYUCCA6	*Potri.018G036800.1*	*AT5G25620.1*	*AtYUCCA6*	5.32	nd	Catalyzes conversion of IPyA to IAA
PtaGH3-1	*Potri.007G050300.1*	*AT2G14960.1*	*AtGH3-1*	2.04	3,969	IAA-amino synthase enzyme
PtaGH3-2	*Potri.009G092900.1*	*AT2G14960.1*	*AtGH3-1*	2.95	1,688	IAA-amino synthase enzyme
PtaGH3-7	*Potri.001G069000.1*	*AT1G28130.1*	*AtGH3-17*	−2.32	4,695	IAA-amino synthase enzyme
	Potri.005G178900.1	*AT1G44350.1*	*AtILL8*	4.15	1,882	IAA amino acid conjugate hydrolase
Polar auxin carriers						
PtaPIN3a	*Potri.010G112800.1*	*AT1G70940.1*	*AtPIN3*	5.83	nd	IAA efflux carrier
PtaPIN3b	*Potri.008G129400.1*	*AT1G70940.1*	*AtPIN3*	4.86	nd	IAA efflux carrier
PtaPIN1c	*Potri.006G037000.1*	*AT1G73590.1*	*AtPIN1*	3.44	1,135	IAA efflux carrier
PtaPIN2	*Potri.018G139400.1*	*AT5G57090.1*	*AtPIN2*	−6.76	5,209	IAA efflux carrier
PtaAUX8/LAX4	*Potri.002G087000.1*	*AT1G77690.1*	*AtLAX3*	−3.26	6,614	IAA influx carrier
PtaAUX8/LAX8	*Potri.005G174000.1*	*AT1G77690.1*	*AtLAX3*	−3.01	8,993	IAA influx carrier
PtaAUX2/LAX1	*Potri.016G113600.1*	*AT2G38120.1*	*AtAUX1*	5.84	nd	IAA influx carrier
PtaABCB5	*Potri.010G003000.1*	*AT2G47000.1*	*AtABCB4*	−3.15	5,912	IAA efflux/influx carrier
PtaABCB19	*Potri.017G081100.1*	*AT3G28860.1*	*AtABCB19*	2.76	432	IAA efflux carrier

[a]Gene name as referred to in Phytozome or named by Kalluri et al. (2007), Felten et al. (2009), Carraro et al. (2012), and Liu et al. (2014). [b]Gene identifier from the *P. trichocarpa* genome version 3.0. [c]Arabidopsis gene identifier and name ortholog to *P. trichocarpa* gene identifier (Phytozome annotation). [d]Fold change of the fluorescence level in mycorrhiza roots compared with control roots. [e]Level of fluorescence in the control roots. [f]Literature annotation in the function of the protein associate.

PCR analysis of a different set of samples, whereas no differential expression was found for *PtaIAA3.3* in this experiment (Supplemental Fig. S3). Overall, our transcriptome analysis identified several auxin-related genes differentially expressed in mature ECM.

DISCUSSION

The development of short and swollen LRs induced by fungal colonization during ECM formation is a well-known phenotype, but the underlying molecular mechanisms that regulate this phenomenon are poorly understood. In this study, we showed that the colonization of *Populus* spp. roots by *L. bicolor* led to growth arrest of LRs and ARs. We characterized the concomitant changes in the auxin metabolome, auxin response, and auxin-related transcriptome.

L. bicolor Colonization Generates an Auxin-Rich Environment in *Populus* spp. Roots Influencing Root Growth

Analysis of IAA-related metabolite concentrations (Fig. 3) revealed that compounds from only two of the four known Trp-dependent IAA biosynthesis pathways involving the IPyA and TRA metabolites accumulated in *P. tremula* × *P alba* roots. This suggest that Trp-dependent IAA biosynthesis in *P. tremula* × *P. alba* occurs mainly via the TRA and IPyA pathways, similar to what has been described in other plant species (Sugawara et al., 2009; Novák et al., 2012; Ljung, 2013). IAAsp and IAGlu were detected in control root, suggesting that IAA conjugation occurs during *Populus* spp. root development. *L. bicolor* mycelium contained high levels of IAA and the IAA precursor IPyA, highlighting that the IPyA pathway seems to be the predominant IAA biosynthesis pathway in *L. bicolor*

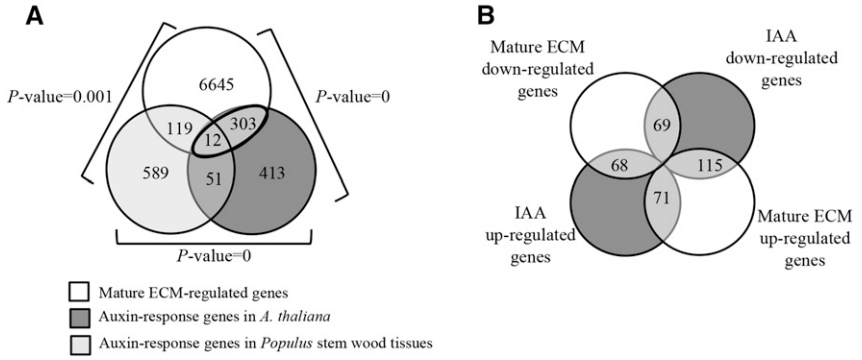

Figure 5. Expression patterns of auxin-response genes in mature ECM. A, Venn diagram illustrating differentially expressed transcripts in mature ECM of *P. tremula* × *P. alba* homologs of Arabidopsis genes responding to auxin (Nemhauser et al., 2006) and of *Populus* spp. wood-forming tissues responding to auxin (Nilsson et al., 2008). Genes were considered to be differentially expressed at greater than 2-fold change and Benjamini and Hochberg-corrected ANOVA $P < 0.05$. Randomization tests were performed between each pair of gene lists, and the resulting *P* value is noted outside the square brackets. B, Venn diagram illustrating the number of differentially regulated transcripts in mature ECM (white area) compared with *Populus* spp. homologs of Arabidopsis auxin-response genes (Nemhauser et al., 2006; dark gray area). Light gray shading indicates the number of genes regulated in the same or opposite ways by IAA and ECM development, respectively.

mycelium. Interestingly, unlike oxIAA, IAA conjugation products were not detected in free-living *L. bicolor* mycelium, suggesting that the IAA balance is regulated by biosynthesis and IAA degradation only.

The multivariate analysis of auxin-related metabolite concentrations (Fig. 4) revealed elevated concentrations of IAA and its precursors ANT, Trp, and IPyA in mature ECM. The in planta IPyA-dependent pathway was activated when host roots were in indirect contact with *L. bicolor* (through a permeable membrane). Together, these findings suggest that IAA biosynthesis in planta could be involved in the accumulation of IAA in mature ECM roots, with concomitant changes in auxin homeostasis in host roots. Since IAA conjugation has not been detected in free-living *L. bicolor* mycelium, not even when the cultures were supplemented with exogenous IAA, the higher IAAsp concentration observed in mature ECM (Supplemental Table S1) could be due to activation of the IAA conjugation pathway in *Populus* spp. root cells. This hypothesis is supported by evidence that IAAsp and IAGlu metabolites accumulate in host plants in indirect contact with *L. bicolor*. Consistent with this observation, the expression levels of *PtaGH3-1* and *PtaGH3-2* were increased in mature ECM. PtaGH3-1 and PtaGH3-2 protein sequences show homology with Arabidopsis group II AtGH3 proteins (Felten et al., 2009), which are considered to be IAA-amino synthases that conjugate IAA to amino acids (Staswick et al., 2005). The *PtaGH3-1* expression level was induced as early as 3 d after coculture with *L. bicolor* (Felten et al., 2009). The auxin conjugation pathway is known to regulate auxin homeostasis and is activated in response to exogenous auxin (Ljung, 2013; Supplemental Fig. S2). We propose that the elevated concentration of IAA conjugates in ECM results from an increase in IAA conjugation through an activation of *GH3* genes. Also, IAA catabolism is induced during colonization of the root and is visible through the accumulation of oxIAA in response to indirect contact with *L. bicolor* and in colonized roots and ECM (Fig. 4; Supplemental Table S1). The accumulation of oxIAA has been described previously as a typical response to high IAA levels (Pencík et al., 2013).

The increase in auxin levels in colonized roots might contribute to the arrest of root growth. Additionally, the concentrations of IAA and its precursors were higher in ECM than in control LRs. It is known that optimal IAA levels are required for the regulation of root growth (Thimann, 1938), and our results suggest that ECM roots contain suboptimal endogenous auxin that inhibits root growth. Moreover, as in other species, ECM *Populus* spp. root apices show drastic changes in cell and tissue organization, including a reduction of the root cap and of the meristem. These developmental changes could be due to an impairment of auxin responses and to an auxin-rich environment in ECM.

L. bicolor Colonization Triggers Symbiosis-Dependent Auxin Signaling

Our expression analysis of *DR5*::*GUS* in roots revealed a progressive decrease in the DR5 auxin response during ECM establishment (Fig. 2), which is consistent with a previous study showing the decrease of *GH3*::*GUS* transcripts in *P. canescens-P. involutus* ECM (Luo et al., 2009). A similarly drastic decrease in *DR5*::*GUS* expression was observed in Arabidopsis roots at low phosphorus availability and was correlated with a decrease in meristematic activity and thus root growth arrest (López-Bucio et al., 2003). The

decrease in the DR5 auxin response could also be correlated with the progressive root growth arrest observed during ECM formation (Fig. 1). IAA or NAA application did not change the GUS expression pattern on ECM root apices. This unexpected observation suggests that the root response to auxin is impaired during colonization by *L. bicolor*, possibly due to a loss of sensitivity to (fungal) auxin. Our transcript profiling revealed a significant repression in expression levels of members of the auxin-response *PtaAux/IAA* family (Table I). Conversely, the expression of several auxin-signaling genes was induced and half of the auxin-response genes that are up-regulated in mature ECM did not respond as expected (Fig. 5). In Arabidopsis, the network of combinatorial interactions between six TIR1/AFBs, 29 Aux/IAAs, and 23 ARFs may result in a large variety of coreceptors with distinct auxin-sensing properties contributing to the complexity of the auxin response (Vernoux et al., 2011; Calderón-Villalobos et al., 2012). The regulation of *PtaAFB5*, *PtaAux/IAA*, and *PtaARF* genes in mature ECM could establish a symbiosis-specific auxin response, which in consequence leads to the root growth arrest.

Interestingly, the up-regulation of a gene coding for a putative nondegradable transcription regulator of auxin signaling, *PtaAux/IAA20.2*, ortholog of *AtAux/IAA30* (Sato and Yamamoto, 2008), was observed in mature ECM. One hypothesis is that the plant regulates by itself the nonresponse to auxin by overexpression of nondegradable *Aux/IAAs*. Also, the overexpression of this *AuxIAA* in Arabidopsis leads to a severe phenotype, including primary root growth arrest due to the collapse of the root apical meristem (Sato and Yamamoto, 2008). As a second hypothesis, the auxin-signaling pathway is likely to be the target of unknown diffusible signals such as effectors, volatile organic compounds (Ditengou et al., 2015), and/or hormones released by *L. bicolor*. ECM development in *L. bicolor* mycelium triggers the induction of genes coding for small secreted proteins (Martin et al., 2008). The protein MYCORRHIZA-INDUCED SMALL SECRETED PROTEIN OF 7 kD (MISSP7) secreted by *L. bicolor* enters the nucleus of epidermal cells and thus regulates specific gene expression, including that of auxin-associated genes in *Populus* spp. (Plett et al., 2011). MISSP7 physically interacts with PtaPtJAZ6, the jasmonate coreceptor, altering the jasmonate signaling pathways (Plett et al., 2014). Recently, an *L. bicolor* volatile organic compound in the sesquiterpenes group was identified as a signal molecule emitted by the fungi to modified root architecture (Ditengou et al., 2015). Future work will aim to investigate whether and which *L. bicolor* signals specifically regulate *PtaAFB5*, *PtaAux/IAA*, and *PtaARF* transcript expression in planta.

CONCLUSION

Concentrations of key auxin metabolites indicate that ECM roots develop in an auxin-rich environment with alterations in auxin metabolism in both partners as symbiosis is establishing. The transcriptome and the *DR5* expression in mature ECM underwent dramatic changes that could be viewed as an implementation of a distinct auxin-signaling network. Based on the results presented here, we propose a working model to illustrate the impact of signaling pathways on the auxin-signaling and -response pathways implemented during the development of *Populus* spp.-*L. bicolor* ECM (Fig. 6). (1) Auxin is synthesized in hyphae in contact with LRs, secreted, and transferred to root cells, where it triggers host auxin-signaling pathways. This contributes to colonization of the root tissues and leads to the observed root growth arrest. The high level of *PtaGH3* expression, as part of this auxin response, would activate the production of IAA-amino synthases and, therefore, lead to the accumulation of IAA conjugates with amino acids. Considering that part of the auxin response is repressed in *Populus* spp. roots and that ECM roots lose their DR5-related responsiveness, we suggest that (2) the plant autoregulates auxin signaling by the overexpression of nondegradable *Aux/IAA* or (3) another unknown signal from *L. bicolor* exudates or diffusible molecules regulate the symbiosis-specific auxin signaling by modifying the expression of *PtaAFB5*, *PtaAux/IAA*, and *PtaARF* genes in the ECM root.

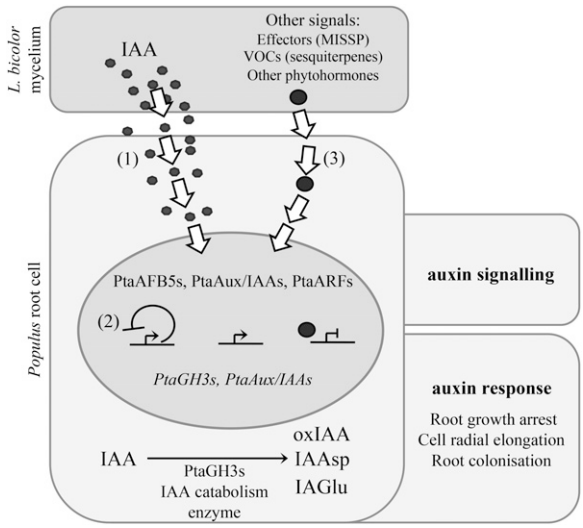

Figure 6. Working model illustrating the modification of *Populus* spp. auxin signaling and metabolism during the colonization of *L. bicolor*. Auxin produced and secreted by *L. bicolor* hyphae (1) activates auxin-signaling pathways in the host plant and contributes to root growth arrest. The auxin response observed in the host plant could be explained by (2) the self-regulation of auxin signaling. The existence of an unidentified signal secreted by *L. bicolor* (3) might also hijack the auxin-signaling pathway, inducing a specific auxin-signaling pathway in the host, leading to root growth arrest. Changes in auxin-signaling pathways are associated with auxin metabolism changes, including auxin degradation (oxIAA) and conjugation (IAAsp and IAGlu) pathways. VOCs, Volatile organic compounds.

MATERIALS AND METHODS

Plant and Fungal Material and Growth Conditions

ECM experiments were performed with the hybrid *Populus tremula* × *Populus alba* (line INRA 717-1-B4) or the transgenic hybrid aspen *Populus tremula* × *Populus tremuloides* DR5::GUS line kindly provided by R.P. Bhalerao (Umea Plant Science Centre). Plants were micropropagated in vitro and grown on one-half-strength Murashige and Skoog (MS/2) medium in glass culture tubes in growth chambers at 24°C with a 16-h photoperiod. The dikaryotic vegetative mycelium of strain S238N of the ectomycorrhizal fungus *Laccaria bicolor* was maintained on modified Pachlewski agar medium P5 at 25°C in the dark (Deveau et al., 2007). For in vitro coculture of *Populus* spp. with *L. bicolor*, we used the sandwich system described by Felten et al. (2009). Briefly, rooted stem cuttings from in vitro-grown *Populus* spp. plants were transferred to petri dishes containing a sugar-reduced Pachlewski agar medium covered with a cellophane membrane. The mycelium-covered cellophane membrane was placed on the roots fungus side down (for direct interaction) or fungus side up (for indirect interaction). Petri dishes for cocultures were positioned vertically with the lower part of the dish covered with black plastic foil. In parallel, vegetative free-living mycelium of *L. bicolor* was grown in the absence of the host plant in darkness for 10 d on a cellophane-covered agar plate containing a sugar-reduced Pachlewski medium (Deveau et al., 2007).

Analysis of Root Growth

LR and AR lengths of eight individual plants (two or three per petri dish) were measured from images of scanned (Epson Perfection V700 PHOTO) culture plates using ImageJ software (http://rsb.info.nih.gov/ij/) with the SMART ROOT plugin (Lobet et al., 2011). Root lengths were measured 0, 1, 2, or 3 weeks after coculture with or without *L. bicolor* mycelium.

Observation of *DR5*::*GUS* Expression

The entire root system of control plants or plants grown in coculture with *L. bicolor* for 2 weeks was sampled and submerged in 5 mL of GUS staining solution under a moderate vacuum (Scarpella et al., 2004). After incubation at 37°C in the dark for a maximum of 2 h, GUS activity was analyzed either in the whole root or from sections of roots. Sections of 30 to 60 μm were made with a vibratome from roots immobilized on 6% (w/v) agarose slides. For the auxin treatments, plants were incubated in a new liquid MS/2 medium for 16 h prior to the addition of 10 μM IAA (Sigma-Aldrich) or 10 μM NAA (Sigma-Aldrich) for an additional 16 h. Plants were washed three times with MS/2 medium and once with distilled water before GUS staining. Representative photographs from two different biological experiments were taken using a Canon digital camera (EOS 350) and a Discovery V.8 stereomicroscope (Zeiss). Areas of GUS staining were measured using ImageJ software.

Quantification of IAA Metabolites

One-centimeter root tips of *Populus* spp. plants were harvested from LRs of plants grown for 1 week in direct or indirect coculture, 3 weeks in coculture, and associated control LRs. Five to six replicates of 20 mg of fresh tissue, representing about 25 root apices, were collected. *L. bicolor* extramatrical mycelium (i.e. mycelium growing within 1 cm of ECM roots) was harvested after 1 and 3 weeks of coculture. In controls, five replicates of 20 mg of *L. bicolor* free-living mycelium, grown for 10 d on Pachlewski agar medium with or without 10 μM IAA (Sigma-Aldrich), were also harvested. *Populus* spp. leaves were harvested in 3-week-old in vitro plants. All samples were weighed, frozen in liquid nitrogen, and kept at −80°C. IAA and its metabolites were quantified by liquid chromatography/multiple reaction monitoring/mass spectrometry (Novák et al., 2012).

RNA Extraction and Complementary DNA Synthesis

For oligoarray transcript profiling and quantitative reverse transcription-PCR analyses, three pools of six individual *P. tremula* × *P. alba* LRs or ECM roots (after 3 weeks of coculture with *L. bicolor*) were harvested in two independent sets, immediately frozen in liquid nitrogen, and then stored at −80°C until RNA extraction. For the analysis of IAA-dependent response genes in *Populus* spp., the root systems of 3-week-old plants were incubated in a new liquid MS/2 medium for 16 h prior to the addition of 10 μM IAA (Sigma-Aldrich) in MS/2 liquid medium for 2 or 6 h. Roots were then washed three times with MS/2 medium and once with water, immediately frozen in liquid nitrogen, then kept at −80°C before RNA extraction. Total RNA was extracted using the RNeasy Plant Mini Kit (Qiagen) following the manufacturer's instructions, including an on-column digestion step with DNase I (Qiagen). RNA quality and quantity were assayed before complementary DNA (cDNA) synthesis using Experion StdSens or HighSens capillary gels (Bio-Rad). The DNA content in RNA samples was tested by quantitative real-time PCR using PtaUBIQUITIN primers (see "Quantitative Real-Time PCR" below). The cDNAs used for the NimbleGen microarrays were synthesized and amplified using the SMARTer PCR cDNA Synthesis Kit (Clontech) according to the manufacturer's instructions. The cDNA used for real-time PCR was synthesized using the iScript Kit (Bio-Rad).

Oligoarray-Based Transcript Profiling

A whole-genome expression oligoarray manufactured by NimbleGen Systems based on the *Populus trichocarpa* gene annotation was used (Gene Expression Omnibus platform GPL13485). This oligoarray contained three independent, nonidentical 60-mer probes from 43,929 annotated gene models of the *P. trichocarpa* genome version 2 (Phytozome 5.0). The genome version and gene names of *P. trichocarpa* were revised at the end of 2012 while this work was being carried out, so we added a column in Supplemental Table S2 that provides the new gene identifiers (*P. trichocarpa* genome version 3; Phytozome 10.1). Single-dye labeling of samples, hybridization procedures, and data acquisition were all performed at the NimbleGen facilities following their standard protocol. Three biological replicates were performed for each condition. Microarray probe intensities were normalized across arrays using ARRAYSTAR software (DNASTAR). Natural log-transformed data were calculated and processed in the Cyber-T statistical framework (http://www.r-project.org/) using the one-way ANOVA multiple condition and the standard Student's *t* test unpaired two-condition data modules. ANOVA was followed by Tukey's honestly significant difference pairwise posthoc tests. Benjamini and Hochberg multiple-hypothesis testing correction with false discovery rate was used for both the ANOVA and the Student's *t* test. Transcripts with a *q* value (Bayesian posterior *P* value) of less than 0.05 for the Benjamini and Hochberg test of expression differences between the two sets of microarray analyses were considered to be significantly different. Randomly designed probes present on the array were used to estimate nonspecific hybridization. In addition, in order to avoid artifacts, we filtered out rare transcripts with expression levels below 300. The *Populus* spp. genome contains a large number of duplicated genes, so we added a column in Supplemental Table S2 to indicate the genes in which all three probes risk to cross hybridize with several transcripts. In our analyses, we focused on genes with a greater than 2-fold change in transcript level. The complete transcriptome data set is available as series GSE66237 at the Gene Expression Omnibus at the National Center for Biotechnology Information (http://www.ncbi.nlm.nih.gov/geo/).

Quantitative Real-Time PCR

We confirmed that the ubiquitin-coding genes *PtUBQ* (*Potri.015G013600.1*; Gutierrez et al., 2008) and *Putative Cytoskeleton Protein* (*Potri.009G093200.1*; Kohler et al., 2004) could be used as reference genes, as their expression was not significantly modified in LRs compared with ECM roots (Felten et al., 2009). QuantPrime software (Arvidsson et al., 2008) was used to design specific primer pairs for the target genes not described by Felten et al. (2009). Quantitative real-time PCR was performed using SYB Green Supermix (Bio-Rad) following the manufacturer's instructions, a Chromo4 Light Cycler, and OpticonMonitor software (Bio-Rad). The analysis was performed on three biological replicates. Three technical replicates were prepared using 2.5 ng of cDNA for each reaction. The cycle number at which the fluorescence crosses the threshold is called the Ct value. This threshold was placed at 0.1 for all genes tested. The relative gene expression values were based on ΔCt calculations using the mean of the two reference gene expression values, according to Pfaffl (2001). The ΔCt values were scaled to the average for the control condition and transformed to $\log_2$. Means of the three values are shown with their SE values. Student's *t* tests associated with *F* tests were performed using Microsoft Office Excel.

Statistical Analysis

IAA-related metabolite concentrations of different organisms were analyzed using a principal component analysis performed with R software (http://r-project.org/) computed using the ade4 package (Chessel et al., 2004).

For the randomization test on transcript profiling, we used the annotation of hormone-response genes described in *Populus* spp. stem wood tissues (Nilsson et al., 2008) and by Nemhauser et al. (2006) for Arabidopsis (*Arabidopsis thaliana*). We used the Phytozome annotation to identify Arabidopsis orthologs of *P. trichocarpa* genes from the oligoarray data (Supplemental Table S4). We assumed that *Populus* spp. orthologs of Arabidopsis hormone-response genes respond to hormones in the same way. Data processing was performed with R software. As described previously by Krouk et al. (2010), we tested whether the overlap between two sets of genes was higher than would be expected by chance. The test consists of randomly selecting 10,000 genes from the *Populus* spp. gene set present on the oligoarray. We thus counted the number (n) of times that the intersection size of the random lists was equal to or higher than the intersection observed for two lists of tested genes. A P value of $n/10{,}000$ was calculated.

Supplemental Data

The following supplemental materials are available.

Supplemental Figure S1. Auxin-related metabolites in *L. bicolor* mycelium grown on medium-containing IAA.

Supplemental Figure S2. Expression of *PtaGH3-1*, *PtaIAA3.3*, *PtaIAA20.2*, and *PtaIAA28.1* in *P. tremula* × *P. alba* root in response to IAA.

Supplemental Figure S3. Relative expression of *PtaGH3-1*, *PtaIAA3.3*, *PtaIAA20.2*, *PtaIAA28.1*, *PtaIAA12.1*, and *PtaIAA3.4* in ECM roots.

Supplemental Table S1. Mean concentrations of auxin related-metabolites in the different tissues.

Supplemental Table S2. List of genes whose transcript levels changed in 3-week-old ECM *P. tremula* × *P. alba* roots in comparison with control LRs.

Supplemental Table S3. Genes related to GA, brassinosteroids, and cytokinin signaling and metabolism differentially regulated in mature ECM in comparison with control LRs and identified in Arabidopsis as regulating root meristem size (Depuydt and Hardtke, 2011).

Supplemental Table S4. List of genes whose transcript levels changed in response to auxin and in 3-week-old ECM.

ACKNOWLEDGMENTS

We thank Jean Pierre Lecler and Patrice Vion for technical assistance; Irène Hummel, Marie-Béatrice Bogeat-Triboulot, Claire Veneault-Fourrey, Adeline Rigal, Stéphanie Robert, Catherine Bellini, and Franck A. Ditengou for helpful discussions; and Rishikesh Bhalerao for providing *DR5*::*GUS* lines.

Received December 17, 2014; accepted June 11, 2015; published June 17, 2015.

LITERATURE CITED

Arvidsson S, Kwasniewski M, Riaño-Pachón DM, Mueller-Roeber B (2008) QuantPrime: a flexible tool for reliable high-throughput primer design for quantitative PCR. BMC Bioinformatics **9:** 465

Burgess T, Dell B, Malajczuk N (1996) *In vitro* synthesis of *Pisolithus-Eucalyptus* ectomycorrhizae: synchronization of lateral tip emergence and ectomycorrhizal development. Mycorrhiza **6:** 189–196

Calderón-Villalobos LI, Lee S, De Oliveira C, Ivetac A, Brandt W, Armitage L, Sheard LB, Tan X, Parry G, Mao H, et al (2012) A combinatorial TIR1/AFB-Aux/IAA co-receptor system for differential sensing of auxin. Nat Chem Biol **8:** 477–485

Carraro N, Tisdale-Orr TE, Clouse RM, Knöller AS, Spicer R (2012) Diversification and expression of the PIN, AUX/LAX, and ABCB families of putative auxin transporters in *Populus*. Front Plant Sci **3:** 17–37

Charvet-Candela V, Hitchin S, Ernst D, Sandermann H, Marmeisse R, Gay G (2002) Characterization of an Aux/IAA cDNA upregulated in *Pinus pinaster* roots in response to colonization by the ectomycorrhizal fungus *Hebeloma cylindrosporum*. New Phytol **154:** 769–777

Chessel D, Dufour AB, Thioulouse J (2004) The ade4 package. I . One-table methods. R News **4:** 5–10

Depuydt S, Hardtke CS (2011) Hormone signalling crosstalk in plant growth regulation. Curr Biol **21:** R365–R373

Deveau A, Palin B, Delaruelle C, Peter M, Kohler A, Pierrat JC, Sarniguet A, Garbaye J, Martin F, Frey-Klett P (2007) The mycorrhiza helper *Pseudomonas fluorescens* BBc6R8 has a specific priming effect on the growth, morphology and gene expression of the ectomycorrhizal fungus *Laccaria bicolor* S238N. New Phytol **175:** 743–755

Dharmasiri N, Dharmasiri S, Estelle M (2005) The F-box protein TIR1 is an auxin receptor. Nature **435:** 441–445

Ditengou FA, Béguiristain T, Lapeyrie F (2000) Root hair elongation is inhibited by hypaphorine, the indole alkaloid from the ectomycorrhizal fungus *Pisolithus tinctorius*, and restored by indole-3-acetic acid. Planta **211:** 722–728

Ditengou FA, Müller A, Rosenkranz M, Felten J, Lasok H, van Doorn MM, Legué V, Palme K, Schnitzler JP, Polle A (2015) Volatile signalling by sesquiterpenes from ectomycorrhizal fungi reprogrammes root architecture. Nat Commun **6:** 6279

Dreher KA, Brown J, Saw RE, Callis J (2006) The *Arabidopsis* Aux/IAA protein family has diversified in degradation and auxin responsiveness. Plant Cell **18:** 699–714

Felten J, Kohler A, Morin E, Bhalerao RP, Palme K, Martin F, Ditengou FA, Legué V (2009) The ectomycorrhizal fungus *Laccaria bicolor* stimulates lateral root formation in poplar and Arabidopsis through auxin transport and signaling. Plant Physiol **151:** 1991–2005

Flores-Monterroso A, Canales J, de la Torre F, Ávila C, Cánovas FM (2013) Identification of genes differentially expressed in ectomycorrhizal roots during the *Pinus pinaster-Laccaria bicolor* interaction. Planta **237:** 1637–1650

Fukaki H, Nakao Y, Okushima Y, Theologis A, Tasaka M (2005) Tissue-specific expression of stabilized SOLITARY-ROOT/IAA14 alters lateral root development in Arabidopsis. Plant J **44:** 382–395

Gay G, Normand L, Marmeisse R, Sotta B, Debaud JC (1994) Auxin overproducer mutants of *Hebeloma cylindrosporum* Romagnesi have increased mycorrhizal activity. New Phytol **128:** 645–657

Gutierrez L, Mauriat M, Guénin S, Pelloux J, Lefebvre JF, Louvet R, Rusterucci C, Moritz T, Guerineau F, Bellini C, et al (2008) The lack of a systematic validation of reference genes: a serious pitfall undervalued in reverse transcription-polymerase chain reaction (RT-PCR) analysis in plants. Plant Biotechnol J **6:** 609–618

Heller G, Lundén K, Finlay RD, Asiegbu FO, Elfstrand M (2012) Expression analysis of Clavata1-like and Nodulin21-like genes from *Pinus sylvestris* during ectomycorrhiza formation. Mycorrhiza **22:** 271–277

Horan DP, Chilvers GA, Lapeyrie FF (1988) Time sequence of the infection process in eucalypt ectomycorrhizas. New Phytol **109:** 451–458

Kalluri UC, Difazio SP, Brunner AM, Tuskan GA (2007) Genome-wide analysis of Aux/IAA and ARF gene families in *Populus trichocarpa*. BMC Plant Biol **7:** 59

Karabaghli C, Frey-Klett P, Sotta B, Bonnet M, Le Tacon F (1998) In vitro effects of *Laccaria bicolor* S238N and *Pseudomonas fluorescens* strain BBc6 on rooting of de-rooted shoot hypocotyls of Norway spruce. Tree Physiol **18:** 103–111

Kepinski S, Leyser O (2005) The Arabidopsis F-box protein TIR1 is an auxin receptor. Nature **435:** 446–451

Kohler A, Blaudez D, Chalot M, Martin F (2004) Cloning and expression of multiple metallothioneins from hybrid poplar. New Phytol **164:** 83–93

Krouk G, Mirowski P, LeCun Y, Shasha DE, Coruzzi GM (2010) Predictive network modeling of the high-resolution dynamic plant transcriptome in response to nitrate. Genome Biol **11:** R123

Liu B, Zhang J, Wang L, Li J, Zheng H, Chen J, Lu M (2014) A survey of Populus PIN-FORMED family genes reveals their diversified expression patterns. J Exp Bot **65:** 2437–2448

Ljung K (2013) Auxin metabolism and homeostasis during plant development. Development **140:** 943–950

Lobet G, Pagès L, Draye X (2011) A novel image-analysis toolbox enabling quantitative analysis of root system architecture. Plant Physiol **157:** 29–39

López-Bucio J, Cruz-Ramírez A, Herrera-Estrella L (2003) The role of nutrient availability in regulating root architecture. Curr Opin Plant Biol **6:** 280–287

Ludwig-Müller J (2011) Auxin conjugates: their role for plant development and in the evolution of land plants. J Exp Bot **62:** 1757–1773

Luo ZB, Janz D, Jiang X, Göbel C, Wildhagen H, Tan Y, Rennenberg H, Feussner I, Polle A (2009) Upgrading root physiology for stress tolerance by ectomycorrhizas: insights from metabolite and transcriptional

profiling into reprogramming for stress anticipation. Plant Physiol **151:** 1902–1917

Martin F, Aerts A, Ahrén D, Brun A, Danchin EGJ, Duchaussoy F, Gibon J, Kohler A, Lindquist E, Pereda V, et al (2008) The genome of *Laccaria bicolor* provides insights into mycorrhizal symbiosis. Nature **452:** 88–92

Martin F, Nehls U (2009) Harnessing ectomycorrhizal genomics for ecological insights. Curr Opin Plant Biol **12:** 508–515

Massicotte HB, Peterson RL, Ashford AE (1987) Ontogeny of *Eucalyptus pilularis-Pisolithus tinctorius* ectomycorrhizae. I. Light microscopy and scanning electron microscopy. Can J Bot **65:** 1927–1939

Nemhauser JL, Hong F, Chory J (2006) Different plant hormones regulate similar processes through largely nonoverlapping transcriptional responses. Cell **126:** 467–475

Niemi K, Vuorinen T, Ernstsen A, Häggman H (2002) Ectomycorrhizal fungi and exogenous auxins influence root and mycorrhiza formation of Scots pine hypocotyl cuttings *in vitro*. Tree Physiol **22:** 1231–1239

Nilsson J, Karlberg A, Antti H, Lopez-Vernaza M, Mellerowicz E, Perrot-Rechenmann C, Sandberg G, Bhalerao RP (2008) Dissecting the molecular basis of the regulation of wood formation by auxin in hybrid aspen. Plant Cell **20:** 843–855

Novák O, Hényková E, Sairanen I, Kowalczyk M, Pospíšil T, Ljung K (2012) Tissue-specific profiling of the *Arabidopsis thaliana* auxin metabolome. Plant J **72:** 523–536

Parizot B, Beeckman T (2013) Genomics of root development. *In* M Crespi, ed, Root Genomics and Soil Interactions. Wiley, New York, pp 3–28

Peer WA, Cheng Y, Murphy AS (2013) Evidence of oxidative attenuation of auxin signalling. J Exp Bot **64:** 2629–2639

Pencík A, Simonovik B, Petersson SV, Henyková E, Simon S, Greenham K, Zhang Y, Kowalczyk M, Estelle M, Zazímalová E, et al (2013) Regulation of auxin homeostasis and gradients in *Arabidopsis* roots through the formation of the indole-3-acetic acid catabolite 2-oxindole-3-acetic acid. Plant Cell **25:** 3858–3870

Pfaffl MW (2001) A new mathematical model for relative quantification in real-time RT-PCR. Nucleic Acids Res **29:** e45

Plett JM, Daguerre Y, Wittulsky S, Vayssières A, Deveau A, Melton SJ, Kohler A, Morrell-Falvey JL, Brun A, Veneault-Fourrey C, et al (2014) Effector MiSSP7 of the mutualistic fungus *Laccaria bicolor* stabilizes the Populus JAZ6 protein and represses jasmonic acid (JA) responsive genes. Proc Natl Acad Sci USA **111:** 8299–8304

Plett JM, Kemppainen M, Kale SD, Kohler A, Legué V, Brun A, Tyler BM, Pardo AG, Martin F (2011) A secreted effector protein of *Laccaria bicolor* is required for symbiosis development. Curr Biol **21:** 1197–1203

Rathnayake AP, Kadono H, Toyooka S, Miwa M (2008) A novel optical interference technique to measure minute root elongations of Japanese red pine (*Pinus densiflora* Seibold & Zucc.) seedlings infected with ectomycorrhizal fungi. Environ Exp Bot **64:** 314–321

Reddy SM, Hitchin S, Melayah D, Pandey AK, Raffier C, Henderson J, Marmeisse R, Gay G (2006) The auxin-inducible GH3 homologue PpGH3.16 is downregulated in *Pinus pinaster* root systems on ectomycorrhizal symbiosis establishment. New Phytol **170:** 391–400

Rincón A, Priha O, Sotta B, Bonnet M, Le Tacon F (2003) Comparative effects of auxin transport inhibitors on rhizogenesis and mycorrhizal establishment of spruce seedlings inoculated with *Laccaria bicolor*. Tree Physiol **23:** 785–791

Rosquete MR, Barbez E, Kleine-Vehn J (2012) Cellular auxin homeostasis: gatekeeping is housekeeping. Mol Plant **5:** 772–786

Sabatini S, Beis D, Wolkenfelt H, Murfett J, Guilfoyle T, Malamy J, Benfey P, Leyser O, Bechtold N, Weisbeek P, et al (1999) An auxin-dependent distal organizer of pattern and polarity in the Arabidopsis root. Cell **99:** 463–472

Sato A, Yamamoto KT (2008) Overexpression of the non-canonical *Aux/IAA* genes causes auxin-related aberrant phenotypes in Arabidopsis. Physiol Plant **133:** 397–405

Scarpella E, Francis P, Berleth T (2004) Stage-specific markers define early steps of procambium development in Arabidopsis leaves and correlate termination of vein formation with mesophyll differentiation. Development **131:** 3445–3455

Smith SE, Read DJ (2008) Mycorrhizal Symbiosis, Ed 3. Academic Press, London

Splivallo R, Fischer U, Göbel C, Feussner I, Karlovsky P (2009) Truffles regulate plant root morphogenesis via the production of auxin and ethylene. Plant Physiol **150:** 2018–2029

Staswick PE, Serban B, Rowe M, Tiryaki I, Maldonado MT, Maldonado MC, Suza W (2005) Characterization of an *Arabidopsis* enzyme family that conjugates amino acids to indole-3-acetic acid. Plant Cell **17:** 616–627

Sugawara S, Hishiyama S, Jikumaru Y, Hanada A, Nishimura T, Koshiba T, Zhao Y, Kamiya Y, Kasahara H (2009) Biochemical analyses of indole-3-acetaldoxime-dependent auxin biosynthesis in Arabidopsis. Proc Natl Acad Sci USA **106:** 5430–5435

Sukumar P, Legué V, Vayssières A, Martin F, Tuskan GA, Kalluri UC (2013) Involvement of auxin pathways in modulating root architecture during beneficial plant-microorganism interactions. Plant Cell Environ **36:** 909–919

Tanaka H, Dhonukshe P, Brewer PB, Friml J (2006) Spatiotemporal asymmetric auxin distribution: a means to coordinate plant development. Cell Mol Life Sci **63:** 2738–2754

Tarkka MT, Herrmann S, Wubet T, Feldhahn L, Recht S, Kurth F, Mailänder S, Bönn M, Neef M, Angay O, et al (2013) OakContigDF159.1, a reference library for studying differential gene expression in *Quercus robur* during controlled biotic interactions: use for quantitative transcriptomic profiling of oak roots in ectomycorrhizal symbiosis. New Phytol **199:** 529–540

Thimann KV (1938) Hormones and the analysis of growth. Plant Physiol **13:** 437–449

Tranvan H, Habricot Y, Jeannette E, Gay G, Sotta B (2000) Dynamics of symbiotic establishment between an IAA-overproducing mutant of the ectomycorrhizal fungus *Hebeloma cylindrosporum* and *Pinus pinaster*. Tree Physiol **20:** 123–129

Ulmasov T, Hagen G, Guilfoyle TJ (1999) Dimerization and DNA binding of auxin response factors. Plant J **19:** 309–319

Vernoux T, Brunoud G, Farcot E, Morin V, Van den Daele H, Legrand J, Oliva M, Das P, Larrieu A, Wells D, et al (2011) The auxin signalling network translates dynamic input into robust patterning at the shoot apex. Mol Syst Biol **7:** 508

Wallander H, Nylund E, Sundberg B (1992) Ectomycorrhiza and nitrogen effects on root IAA: results contrary to current theory. Mycorrhiza **1:** 91–92